The Orbital Selection Rule for Molecular Conductance as Manifested in Tetraphenyl-Based Molecular Junctions

Marius Bürkle,[*,†] Limin Xiang,[‡] Guangfeng Li,[¶] Ali Rostamian,[‡] Thomas Hines,[‡] Shaoyin Guo,[‡] Gang Zhou,[¶] Nongjian Tao,[*,‡] and Yoshihiro Asai[*,†]

[†]National Institute of Advanced Industrial Science and Technology (AIST), Research Center for Computational Design of Advanced Functional Materials (CD-FMat), Central 2, Umezono 1-1-1, Tsukuba, Ibaraki 305-8568, Japan

[‡]Center for Bioelectronics and Biosensors, Biodesign Institute, Arizona State University, Tempe, Arizona 85287, United States

[¶]Laboratory of Advanced Materials, Fudan University, Shanghai 200438, P.R. China

S *Supporting Information*

ABSTRACT: Using two tetraphenylbenzene isomers differing only by the anchoring points to the gold electrodes, we investigate the influence of quantum interference on the single molecule charge transport. The distinct anchor points are realized by selective halogen-mediated binding to the electrodes by formation of surface-stabilized isomers after iodine cleavage. Both isomers are essentially chemically identical and only weakly perturbed by the electrodes avoiding largely parasitic effects, which allows us to focus solely on the relation between quantum interference and the intrinsic molecular properties. The conductance of the two isomers differs by over 1 order of magnitude and is attributed to constructive and destructive interference. Our ab initio based transport calculations compare very well with the accompanying scanning tunneling microscope break junction measurements of the conductance. The findings are rationalized using a two level model, which shows that the interorbital coupling plays the decisive role for the interference effects.
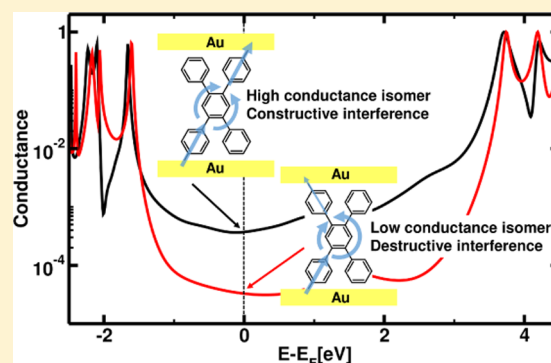
INTRODUCTION

Quantum interference is one of the most fascinating consequences arising from the wave−particle dualism of electrons. First realized by means of the famous double-slit experiment[1,2] and later on in mesoscopic systems,[3] the quantum nature of the electrons was recently also probed in single molecule devices where quantum interference modulates the flow of the electrons through the molecular conductor. Utilizing single-molecule devices is thereby appealing as the transport is usually phase-coherent even at room temperature. The basic idea is that the molecular conductor, similar to classical interferometers, provides different conductance pathways, which can, depending on the phase difference, lead to constructive or destructive interference. This has been recently demonstrated for phenyl rings,[4,5] naphthalenedithiol,[6] and oligo(phenylene ethynylene)[7] derivatives where the conductance of para-contacted molecules is much larger compared to meta-contacted molecules and was also observed for self-assembled monolayers of cross-conjugated molecules.[8,9] From a theoretical point of view, the reduced conductance can be related to the suppression of the transmission due to antiresonances in the vicinity of the Fermi and has been studied, for example, for π-conjugated systems,[10−13] cross-conjugated molecules,[14−16] and linear polyene chains.[12] It is possible to relate the interference effects to the phase difference

along different conductance pathways through the molecule[11,14,17] or equivalently to the orbital symmetry of the molecule, which provides an intuitive qualitative picture for predicting interference effects.[12,18] Here we investigate tetraphenylbenzene (TPB) based molecular junctions, which fall into the class of π-conjugated molecules; namely, we are considering the two isomers displayed in Figure 1, 1,4-bis(4-iodophenyl)-2,5-diphenylbenzene (isomer 1-4) and 1,5-bis(4-iodophenyl)-2,4-diphenylbenzene (isomer 1-5). They differ only in the position of one of the iodine atoms attached to two of the outer benzene rings. After iodine cleavage inside the contact[19−27] and formation of surface stabilized radicals,[28,29] both isomers are essentially chemically identical. This allows us to study quantum interference using an identical molecular framework by simply changing the injection point of the electrons into the molecular conductor. As opposed to the use of side groups or terminal substitution to realize suitable molecular configurations to observe quantum interference, which eventually change the chemical properties of the molecules, we can largely reduce such spurious effects usually superposing the interference effects. We observe consistently in our ab inito based transport calculations and scanning tunneling
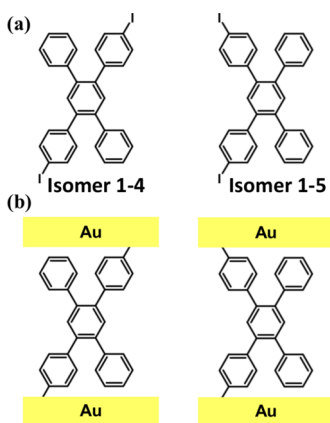
Figure 1. (a) The two considered tetraphenylbenzene derivatives. (b) Covalent junction formation after iodine cleavage by means of surface stabilized radicals.

microscope (STM) break junction (BJ) measurements a large suppression of the conductance of isomer 1-5 as compared to isomer 1-4, which follows the expectation based on Yoshizawa's orbital symmetry rule.[18] Our findings are rationalized using a two level model, which provides a rigorous derivation of the orbital symmetry rule, albeit it remains also valid in the strong coupling case and for on resonant transport and can be readily extended to the multiorbital and multicontact case.

■ THEORETICAL METHOD

The electronic structure of the molecular junction is described within density functional theory (DFT) at the PBE level of theory using the def2-SV(P) basis set and the corresponding Coulomb fitting bases.[30,31] All DFT calculations are carried out with the quantum chemistry package TURBOMOLE.[32] The transport properties are obtained by combining the DFT derived electronic structure with a Green's function formalism including an approximate self-energy correction based on the

DFT + Σ approach accounting for the overestimation of the conductance in DFT based methods.[33,34] In linear response, the conductance G is determined by the electronic transmission probability, $\tau(E_F)$, at the Fermi energy, E_F,

$$G = G_0\tau(E_F) = G_0 \sum \tau_i(E_F) \tag{1}$$

here $G_0 = 2e^2/h$ is the conductance quantum with e being the elementary charge and h the Planck constant. The transmission function $\tau(E) = \mathrm{Tr}[\mathbf{G}^r(E)\mathbf{\Gamma}^L(E)\mathbf{G}^a(E)\mathbf{\Gamma}^R(E)]$ can be expressed in terms of Green's functions, where the Green's functions are defined as $\mathbf{G}^r(E) = [(E + i\eta)\mathbf{S} - \mathbf{H} - \mathbf{\Sigma}^r(E)]^{-1}$ and $\mathbf{G}^a(E) = (\mathbf{G}^r(E))^{\dagger}$ with $\mathbf{H}$ being the Hamilton matrix of the extended molecule and $\mathbf{S}$ the corresponding overlap matrix, $\eta > 0$ an infinitesimal quantity, and $\mathbf{\Sigma}^r(E) = \mathbf{\Sigma}_C^r(E) + \mathbf{\Sigma}_{\mathrm{Mol}}^r(E)$ the self-energy matrix consisting of the contact self-energy $\mathbf{\Sigma}_C^r(E)$ and the DFT+Σ corrections $\mathbf{\Sigma}_{\mathrm{Mol}}^r(E)$, which just acts on the molecular subspace. Moreover it is possible to decompose the transmission $\tau(E_F) = \sum \tau_i(E_F)$ in terms of individual transmission channels τ_i and to calculate the corresponding transmission eigenchannel wave functions Ψ_i as the corresponding eigenstates of the transmission operator $\hat{\tau}|\Psi_i\rangle = \tau_i|\Psi_i\rangle$. A comprehensive discussion of our transport approach can be found in refs 34, 35, and 36. The following discussion will be based on the DFT+Σ results; the pure DFT based transmission spectra along with the parameters used for the DFT+Σ corrections can be found in the Supporting Information (SI).

■ RESULTS

To investigate the influence of the quantum interference on the transport properties, we introduce here a pair of TPB isomers (Figure 1a), which allow us to avoid largely parasitic effects due anchor groups or varying molecular chemistry. After iodine cleavage, the two TPB isomers form stable junctions by means of surface-stabilized radicals (Figure 1b)[19−21,23,25] and can be expected to be essentially chemically identical. This allows us to
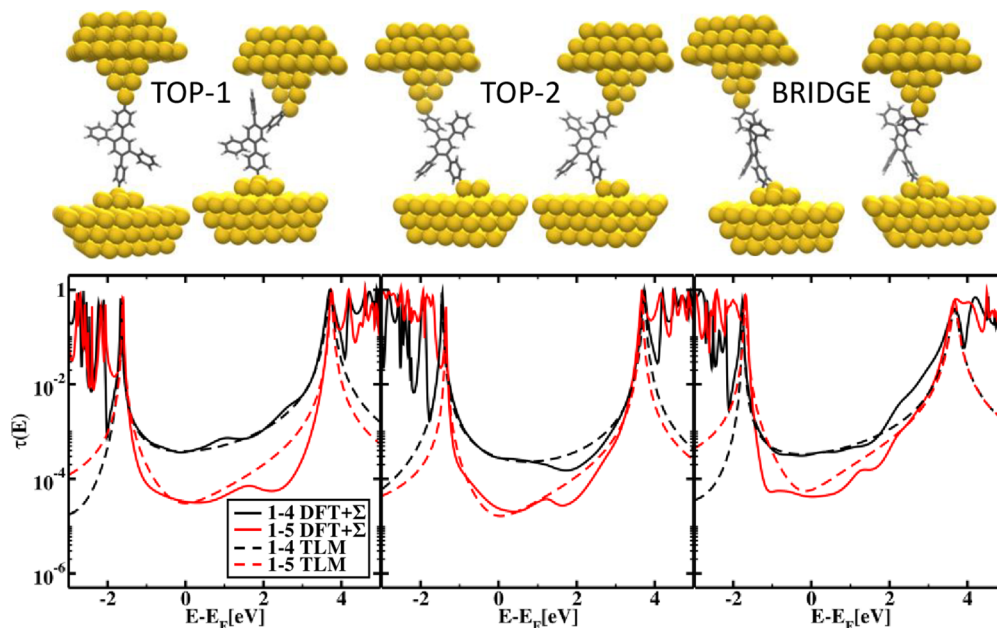

Figure 2. Considered contact geometries and corresponding DFT+Σ based transmission spectra (solid lines) and fitted curves obtained from the two level model (TLM).

directly relate the molecular topology to quantum interference effects.

To account for possible variation of the conductance due to different binding motifs,[36] we consider here three distinct contact geometries (Figure 2), namely, two atop geometries where the molecule binds either to a high-coordinate Au atom (labeled TOP-1) or to low-coordinate Au atom (labeled TOP-2) and a bridge geometry where the molecule binds to two Au atoms (labeled BRIDGE). For all three binding motifs, the intrinsic molecular structure remains mostly identical; thus we do not expect conformation induced variation of the conductance superposing the quantum interference effects. Details on the protocol assumed to construct the junction geometries can be found in SI.

The calculated transmission spectra are given in Figure 2, and the corresponding conductance values are summarized in Table 1. First, we note that the variations between the three contact

Table 1. Calculated and Measured Conductance Values [$10^{-4}G_0$]

isomer	geometry			expt
	TOP-1	TOP-2	BRIDGE	
1-4	3.71	2.86	3.30	3.00
1-5	0.33	0.24	0.41	0.23
G_{1-4}/G_{1-5}	11.2	11.9	8.0	13.0

geometries remain small giving well-defined conductance values for both isomers. As expected, the conductance of the para-contacted isomer 1-4 (constructive interference) is much larger than the conductance of the meta-contacted isomer 1-5 (destructive interference). The relative suppression G_{1-4}/G_{1-5} of the conductance is around 1 order of magnitude. Motivated by our quantitative DFT+Σ based[33] predictions that the two isomers give rise to distinct and well-defined conductance values, we performed conductance measurements for the two TPB isomers using a STM BJ method (Figure S5 in SI). In the relevant conductance range, we observe two well separated peaks in the conductance histogram at $0.23 \times 10^{-4}G_0$ and $3.00 \times 10^{-4}G_0$, which compare very well to the DFT+Σ based predictions of the conductance and G_{1-4}/G_{1-5} ratio for the two isomers. Ruling out the possible formation of molecular wires, π-stacking, and iodine bonding, which all give rise to clearly different conductance values (see SI), we can unambiguously assign the low conductance peak to isomer 1-5 and the high conductance peak to isomer 1-4.

■ DISCUSSION

In the following, we rationalize the ab initio results and discuss the reason for the observed large difference in the conductance of the two isomers. Moreover, we emphasize that the two isomers are indeed largely identical once connected to the electrodes. Several models have been proposed to analyze and predict the occurrence of quantum interference in molecular conductors, for example, by analyzing the different conduction pathways through the molecule[11,14,17,37−39] or by orbital selection rules[12,13,18,40] based on frontier orbital theory.[41,42] Here, the discussion is given in terms of a two level model (TLM) that reproduces, despite its simplicity, the ab initio result very well.

The TLM can be rigorously derived from the spectral decomposition of the transmission function (see SI). The spectral decomposition is generally valid in the multiorbital

case; in the following, however, we are focusing on the two frontier orbitals, that is, the highest occupied molecular orbital (HOMO) and lowest unoccupied molecular orbital (LUMO), of the TPB isomers, which are dominating the transport; contributions from lower and higher lying orbitals,[43,44] which play only a minor part, are neglected. It has to be noted that besides restricting our discussion here to the two frontier orbitals, the TLM remains generally valid; that is, it can be applied for strongly coupled molecules as well as for on-resonant transport. Within the TLM, the transmission is given by (eq S8 in SI)

$$\tau(E) = \frac{\Gamma_{HH}^l \Gamma_{HH}^r}{(E+\epsilon)^2 + \gamma_H^2} + \frac{\Gamma_{LL}^l \Gamma_{LL}^r}{(E-\epsilon)^2 + \gamma_L^2} + 2\frac{\Delta\sqrt{\Gamma_{HH}^l \Gamma_{HH}^r \Gamma_{LL}^l \Gamma_{LL}^r}[E^2 - \epsilon^2 + \gamma_H\gamma_L]}{[(E+\epsilon)^2 + \gamma_H^2][(E-\epsilon)^2 + \gamma_L^2]} \quad (2)$$

where $\epsilon = (\epsilon_L - \epsilon_H)/2$ is determined by the renormalized orbital energy of the two frontier orbitals, $\gamma_X = (\Gamma_{XX}^l + \Gamma_{XX}^r)/2$ is related to the coupling $\Gamma_{XX}^{l,r}$ of the HOMO (X = H) and LUMO (X = L) orbital to electrodes l and r, and $-1 \leq \Delta \leq 1$ gives a measure for the cross coupling between the two frontier orbitals once connected to the electrodes. Essentially Δ determines the phase difference between the scattering phases encountered in the context of the Friedel sum-rule[45,46] leading either to constructive or destructive interference between the scattering states.[47] The sign of $\Delta \approx \Gamma_{HL}^l \Gamma_{HL}^r$ is determined by the cross-terms $\Gamma_{HL}^{l,r} = \langle H|\hat{\Gamma}^{l,r}|L\rangle$, within the HOMO−LUMO gap ($E^2 < \epsilon^2 - \gamma_H\gamma_L$); we get constructive interference for $\Delta < 0$ and destructive interference for $\Delta > 0$. In the limit of weakly coupled molecules and off-resonant transport, as it is the case for the TPB isomers studied here, we can apply the orbital symmetry rule by Yoshizawa and co-workers[10,18,40] and Tsuji and co-workers[12,48] to deduce constructive and destructive interference from the orbital symmetry of the unperturbed molecule, where the orbital symmetry rule can be obtained from the TLM within first-order perturbation theory in the contact self-energy and is valid as long as $\epsilon^2 > \gamma_H\gamma_L$.

Assuming that the left (right) electrode only couples to a single carbon atom l (r), that is, $\Gamma_{HL}^X = \langle H|X\rangle\langle X|\hat{\Gamma}^X|X\rangle\langle X|L\rangle$, the sign of Γ_{HL}^l and Γ_{HL}^r and hence the sign of Δ is solely determined by the relative phase of the molecular orbital coefficients $\langle H|r\rangle$, $\langle r|L\rangle$ and $\langle H|l\rangle$, $\langle l|L\rangle$ (Figure 3), which is equivalent to the statement given by the orbital symmetry rule
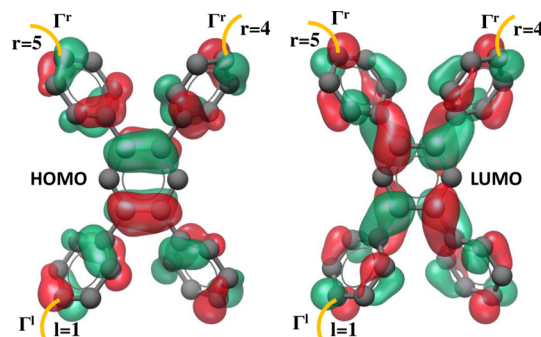

Figure 3. Wave function of the HOMO and LUMO orbitals plotted for the same isosurface value, where red depicts positive and green negative sign of the wave function. The hydrogen on the aromatic benzene rings have been omitted.

of ref 18. Additionally we can obtain all parameters relevant for TLM directly from the full ab initio results; especially we can give a simple measure for the quantum interference in terms of Δ. The parameters are obtained by fitting the TLM to the full DFT+Σ based transmission spectra in the energy range of the HOMO−LUMO gap; orbitals below the HOMO and above the LUMO are not considered. The fits on the TLM, given by the dashed lines in Figure 2, agree reasonably well with the full ab initio results. The corresponding parameters are summarized in Table 2. For all geometries, the cross coupling $|\Delta| \approx 0.75$

Table 2. Parameters Obtained from Fitting the TLM Transmission to the Full DFT Results

	TOP-1		TOP-2		BRIDGE	
	1-4	1-5	1-4	1-5	1-4	1-5
Γ^l_{HH} [meV]	5	6	4	11	15	9
$\Gamma^r_{HH}/\Gamma^l_{HH}$	3.8	3.2	5	2.9	1.5	2.0
Γ^l_{LL} [meV]	53	38	19	25	28	20
$\Gamma^r_{LL}/\Gamma^l_{LL}$	1.0	1.0	7.8	4.0	1.0	1.0
ϵ [eV]	2.69	2.68	2.71	2.68	2.60	2.58
Δ	−0.82	0.75	−0.70	0.80	−0.81	0.78

between the two frontier orbitals remains for the most part independent of the contact geometry. Moreover, for both isomers also the variation of ϵ remains small. Hence, the electronic structure of the frontier orbitals of the surface-passivated isomers 1-4 and 1-5 is indeed largely identical, and the observed variation of the conductance between isomer 1-4 and 1-5 is accordingly mainly caused by interference effects and not by different alignment of the frontier orbitals. This can be illustrated by considering the wave function of the dominating transmission channel (at E_F) originating from the bottom electrode; we see that for both isomers the electrode states couple equally well into the first benzene ring connecting the TPB molecule to Au surface and both wave functions $\Psi_{1\text{-}4}$ and $\Psi_{1\text{-}5}$ decay similarly exponentially along the transport direction (Figure 4) as the decay exponent is in first order independent of the quantum interference[47] and determined by the relative position of ϵ with respect to the electrode Fermi energy.[49−51] However, while the wave function also extends into the benzene ring in para position, its amplitude is due to the destructive interference largely suppressed on the ring in meta position. Lastly, it is worth mentioning that while we focused
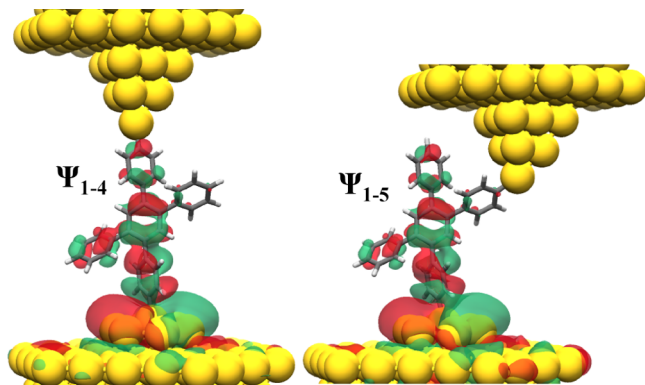

Figure 4. Transmission eigenchannel wave function of the main transmission calculated at the Fermi energy, E_F. Both $\Psi_{1\text{-}4}$ and $\Psi_{1\text{-}5}$ are energy normalized and plotted for the same isosurface value, where red depicts positive and green negative sign (phase) of the wave function.

here on molecules with two well-defined anchor points to obtain clear signatures of constructive and destructive interference avoiding superposition of both effects, an analogous discussion in terms of the TLM can be given for a molecule with multiple contacts points.[16]

CONCLUSION

Using two tetraphenylbenzene isomers differing only by the injection point of the electrons from the contacts, we showed that the different conductance pathways introduced for the two isomers or equivalently orbital symmetry can be directly related to the quantum interference effects on the conductance. The quantum interference can be clearly observed, and both isomers give rise to distinct and well-defined conductance values. The absolute values of the conductance differ by around 1 order of magnitude between both isomers. Motivated by our quantitative DFT+Σ based predictions of the molecular conductance, we performed scanning tunneling microscope break junction based measurements to elucidate the junction formation mechanism. The experimentally observed conductance values compare very well with the theoretical predictions for the covalently bonded tetraphenylbenzene isomers, while they clearly differ for the halogen bonded molecules. This strongly suggests at room temperature a junction formation by covalent Au−C bonds after cleavage of the iodine atoms. Eventually our ab initio results are rationalized in terms of a two level model, which shows that the relative phase between the HOMO and LUMO orbital at the two contacted atoms plays the decisive role for quantum interference and that the variations are clearly attributed to quantum interference and not to parasitic effects superimposing the quantum interference. The simple relation demonstrated here for tetraphenylbenzene derivatives can be readily extended to the multiorbital case and remains valid for the strong coupling case and on resonant transport. In the weak-coupling limit, we recover the recently introduced intuitive orbital symmetry rule, which is consistent with the results obtained here.

ASSOCIATED CONTENT

Ⓢ Supporting Information

The Supporting Information is available free of charge on the ACS Publications website at DOI: 10.1021/jacs.6b10837.

> Details on the modeling of the contact geometries, the parameters used for the DFT+Σ correction, the derivation of the two level model, details on the measurement of the conductance, and the calculated Cartesian coordinates and total energies (PDF)

AUTHOR INFORMATION

Corresponding Authors
*marius.buerkle@aist.go.jp
*nongjian.tao@asu.edu
*yo-asai@aist.go.jp
Notes
The authors declare no competing financial interest.

ACKNOWLEDGMENTS

■ REFERENCES

(1) Jönsson, C. *Eur. Phys. J. A* **1961**, *161*, 454−474.

(2) Merli, P. G.; Missiroli, G. F.; Pozzi, G. *Am. J. Phys.* **1976**, *44*, 306−307.

(3) Liu, R. C.; Odom, B.; Yamamoto, Y.; Tarucha, S. *Nature* **1998**, *391*, 263−265.

(4) Arroyo, C.; Frisenda, R.; Moth-Poulsen, K.; Seldenthuis, J.; Bjornholm, T.; van der Zant, H. *Nanoscale Res. Lett.* **2013**, *8*, 234.

(5) Arroyo, C. R.; Tarkuc, S.; Frisenda, R.; Seldenthuis, J. S.; Woerde, C. H. M.; Eelkema, R.; Grozema, F. C.; van der Zant, H. S. J. *Angew. Chem., Int. Ed.* **2013**, *52*, 3152−3155.

(6) Taniguchi, M.; Tsutsui, M.; Mogi, R.; Sugawara, T.; Tsuji, Y.; Yoshizawa, K.; Kawai, T. *J. Am. Chem. Soc.* **2011**, *133*, 11426−11429.

(7) Manrique, D. Z.; Huang, C.; Baghernejad, M.; Zhao, X.; Al-Owaedi, O. A.; Sadeghi, H.; Kaliginedi, V.; Hong, W.; Gulcur, M.; Wandlowski, T.; et al. *Nat. Commun.* **2015**, *6*, 6389.

(8) Fracasso, D.; Valkenier, H.; Hummelen, J. C.; Solomon, G. C.; Chiechi, R. C. *J. Am. Chem. Soc.* **2011**, *133*, 9556−9563.

(9) Guédon, C. M.; Valkenier, H.; Markussen, T.; Thygesen, K. S.; Hummelen, J. C.; van der Molen, S. J. *Nat. Nanotechnol.* **2012**, *7*, 305−309.

(10) Tada, T.; Yoshizawa, K. *ChemPhysChem* **2002**, *3*, 1035−1037.

(11) Markussen, T.; Stadler, R.; Thygesen, K. S. *Nano Lett.* **2010**, *10*, 4260−4265.

(12) Tsuji, Y.; Hoffmann, R.; Movassagh, R.; Datta, S. *J. Chem. Phys.* **2014**, *141*, 224311.

(13) Tsuji, Y.; Hoffmann, R. *Angew. Chem., Int. Ed.* **2014**, *53*, 4093−4097.

(14) Solomon, G. C.; Andrews, D. Q.; Hansen, T.; Goldsmith, R. H.; Wasielewski, M. R.; Van Duyne, R. P.; Ratner, M. A. *J. Chem. Phys.* **2008**, *129*, 054701.

(15) Solomon, G. C.; Bergfield, J. P.; Stafford, C. A.; Ratner, M. A. *Beilstein J. Nanotechnol.* **2011**, *2*, 862−871.

(16) Hansen, T.; Solomon, G. C. *J. Phys. Chem. C* **2016**, *120*, 6295−6301.

(17) Markussen, T.; Stadler, R.; Thygesen, K. S. *Phys. Chem. Chem. Phys.* **2011**, *13*, 14311−14317.

(18) Yoshizawa, K.; Tada, T.; Staykov, A. *J. Am. Chem. Soc.* **2008**, *130*, 9406−9413.

(19) Syomin, D.; Koel, B. E. *Surf. Sci.* **2001**, *490*, 265−273.

(20) Grill, L.; Dyer, M.; Lafferentz, L.; Persson, M.; Peters, M. V.; Hecht, S. *Nat. Nanotechnol.* **2007**, *2*, 687−691.

(21) Bieri, M.; Nguyen, M.-T.; Gröning, O.; Cai, J.; Treier, M.; Ait-Mansour, K.; Ruffieux, P.; Pignedoli, C. A.; Passerone, D.; Kastler, M.; et al. *J. Am. Chem. Soc.* **2010**, *132*, 16669−16676.

(22) Kanuru, V. K.; Kyriakou, G.; Beaumont, S. K.; Papageorgiou, A. C.; Watson, D. J.; Lambert, R. M. *J. Am. Chem. Soc.* **2010**, *132*, 8081−8086.

(23) Schlögl, S.; Heckl, W. M.; Lackinger, M. *Surf. Sci.* **2012**, *606*, 999−1004.

(24) Lafferentz, L.; Eberhardt, V.; Dri, C.; Africh, C.; Comelli, G.; Esch, F.; Hecht, S.; Grill, L. *Nat. Chem.* **2012**, *4*, 215−220.

(25) Björk, J.; Hanke, F.; Stafström, S. *J. Am. Chem. Soc.* **2013**, *135*, 5768−5775.

(26) Eder, G.; Smith, E. F.; Cebula, I.; Heckl, W. M.; Beton, P. H.; Lackinger, M. *ACS Nano* **2013**, *7*, 3014−3021.

(27) Eichhorn, J.; Nieckarz, D.; Ochs, O.; Samanta, D.; Schmittel, M.; Szabelski, P. J.; Lackinger, M. *ACS Nano* **2014**, *8*, 7880−7889.

(28) Hirayama, M.; Caseri, W. R.; Suter, U. W. *J. Colloid Interface Sci.* **1998**, *202*, 167−172.

(29) Simonet, J.; Jouikov, V. *Electrochem. Commun.* **2014**, *38*, 65−67.

(30) Weigend, F.; Ahlrichs, R. *Phys. Chem. Chem. Phys.* **2005**, *7*, 3297−3305.

(31) Weigend, F. *Phys. Chem. Chem. Phys.* **2006**, *8*, 1057−1065.

(32) TURBOMOLE 6.4, TURBOMOLE GmbH Karlsruhe, http://www.turbomole.com. TURBOMOLE is a development of University of Karlsruhe and Forschungszentrum Karlsruhe 1989−2007, TURBO-MOLE GmbH since 2007.

(33) Quek, S. Y.; Khoo, K. H. *Acc. Chem. Res.* **2014**, *47*, 3250−3257.

(34) Zotti, L. A.; Bürkle, M.; Pauly, F.; Lee, W.; Kim, K.; Jeong, W.; Asai, Y.; Reddy, P.; Cuevas, J. C. *New J. Phys.* **2014**, *16*, 015004.

(35) Pauly, F.; Viljas, J. K.; Huniar, U.; Häfner, M.; Wohlthat, S.; Bürkle, M.; Cuevas, J. C.; Schön, G. *New J. Phys.* **2008**, *10*, 125019.

(36) Bürkle, M.; Viljas, J. K.; Vonlanthen, D.; Mishchenko, A.; Schön, G.; Mayor, M.; Wandlowski, T.; Pauly, F. *Phys. Rev. B: Condens. Matter Mater. Phys.* **2012**, *85*, 075417.

(37) Hansen, T.; Solomon, G. C.; Andrews, D. Q.; Ratner, M. A. *J. Chem. Phys.* **2009**, *131*, 194704.

(38) Kiguchi, M.; Takahashi, Y.; Fujii, S.; Takase, M.; Narita, T.; Iyoda, M.; Horikawa, M.; Naitoh, Y.; Nakamura, H. *J. Phys. Chem. C* **2014**, *118*, 5275−5283.

(39) Lambert, C. J. *Chem. Soc. Rev.* **2015**, *44*, 875−888.

(40) Yoshizawa, K. *Acc. Chem. Res.* **2012**, *45*, 1612−1621.

(41) Fukui, K. *Chemical Reactions and Electron Orbitals*; Maruzen: Tokyo, 1976.

(42) Fleming, I. *Molecular Orbitals and Organic Chemical Reactions*; John Wiley and Sons: Sussex, U.K., 2009.

(43) Pedersen, K. G. L.; Strange, M.; Leijnse, M.; Hedegård, P.; Solomon, G. C.; Paaske, J. *Phys. Rev. B: Condens. Matter Mater. Phys.* **2014**, *90*, 125413.

(44) Strange, M.; Seldenthuis, J. S.; Verzijl, C. J. O.; Thijssen, J. M.; Solomon, G. C. *J. Chem. Phys.* **2015**, *142*, 084703.

(45) Datta, S.; Tian, W. *Phys. Rev. B: Condens. Matter Mater. Phys.* **1997**, *55*, R1914−R1917.

(46) Makoshi, K.; Shima, N.; Otsuka, Y. *Phys. E* **2005**, *29*, 656−659.

(47) Buerkle, M.; Asai, Y. Unpublished work.

(48) Tsuji, Y.; Staykov, A.; Yoshizawa, K. *J. Am. Chem. Soc.* **2011**, *133*, 5955−5965.

(49) Mujica, V.; Kemp, M.; Ratner, M. A. *J. Chem. Phys.* **1994**, *101*, 6856−6864.

(50) Asai, Y.; Fukuyama, H. *Phys. Rev. B: Condens. Matter Mater. Phys.* **2005**, *72*, 085431.

(51) Viljas, J. K.; Pauly, F.; Cuevas, J. C. *Phys. Rev. B: Condens. Matter Mater. Phys.* **2008**, *77*, 155119.